Marine Biology (1995) 124: 399–406

J. H. Costello · S. P. Colin

Flow and feeding by swimming scyphomedusae

Received: 20 June 1995/Accepted: 16 August 1995

Abstract The mechanical basis of prey capture by scyphomedusae has been largely ignored, despite the importance of these predators in a variety of planktonic ecosystems. Interactions between swimming, fluid motions, and prey capture were examined during 1991–1992 for a species from the three scyphozoan orders having planktonic medusae: Rhizostomeae, *Stomolophus meleagris* Agassiz, 1862; Coronatae, *Linuche unguiculata* (Schwartz, 1788); and Semaeostomeae, *Cyanea capillata* (Linnaeus, 1758). All three species used flow created during bell pulsation to capture prey, but the type of flow used for prey capture and the capture surface morphology were different for each species. The mechanics of capture by these species of diverse morphology and taxonomic affinity suggests that the use of bell pulsation-induced flow for prey entrainment and capture is widespread among the scyphomedusae.

Introduction

Scyphomedusae are important predators in a variety of marine communities (Moller 1980a, b, 1984; Lindahl and Hernroth 1983; Matsakis and Conover 1991; Purcell 1992) yet the functional basis for prey selection by scyphomedusae has not been well documented. Previous descriptions of the mechanical bases of medusan prey selection have relied upon tentacle positions of sinking (Mills 1981) or motionless (Madin 1988) medusae, primarily hydrozoans. While applicable to many planktonic coelenterates, models such as these are inappropriate for a number of scyphomedusae, such as those of the order Rhizostomeae, which do not possess tentacles and rarely sit motionless.

An alternative functional model for prey selection by the scyphomedusa, *Aurelia aurita*, was proposed by Costello and Colin (1994). Prey encounters with capture surfaces of *A. aurita* depend upon prey entrainment in fluid motions generated by the swimming medusa. This model predicts that vulnerability of prey to entrainment in medusan flow fields dominates prey selection by *A. aurita*. The utility of this approach for *A. aurita* was demonstrated by Sullivan et al. (1994), who showed that in situ prey selection by *A. aurita* was largely consistent with the flow field model of Costello and Colin (1994). The general applicability of this model to scyphomedusae with widely divergent morphologies may be limited, however, because the model describes prey capture as occurring primarily on the tentacles of *A. aurita*. Analysis of prey capture by several species with different tentacle morphologies is necessary to evaluate the general utility of a flow-based model of prey capture.

Three species of scyphomedusae, representing three types of tentacle morphology and three different scyphomedusan orders, were selected to examine the relationship between swimming, morphology, and prey capture. *Stomolophus meleagris* (Order Rhizostomeae) possesses no tentacles, *Linuche unguiculata* (Order Coronatae) has short tentacles which protrude only slightly beyond the bell margin, and *Cyanea capillata* (Order Semaeostomeae) has long tentacles which may trail below the bell in excess of ten body diameters. We assessed the importance of fluid motions for prey capture by these medusae using the video approach of Costello and Colin (1994).

Methods

Experimental organisms

Stomolophus meleagris Agassiz, 1862 were collected in June 1991 from surface waters at North Inlet, South Carolina, USA and

Communicated by J.P. Grassle, New Brunswick

J.H. Costello (✉) · S.P. Colin
Biology Department, Providence College,
Providence, Rhode Island 02918-0001, USA

shipped by D. Allen to our laboratory in Providence, Rhode Island, USA. *Linuche unguiculata* (Schwartz, 1788) were collected in Bahamian waters during May 1991 and shipped by M. Montgomery and P. Kremer to our laboratory. *Cyanea capillata* (Linnaeus, 1758) were collected in July 1992 from Cape Cod Bay near Brewster, Massachusetts by the authors. Medusae were maintained in the laboratory in incubators at field temperatures (20 to 25 °C) until used for microvideography (within a week of capture).

Microvideography

Activities of medusae, prey and dye were observed using a backlit optical system similar to that described previously (Costello and Colin 1994). A minimum of 3 ind of each species of medusae were videotaped while swimming freely in 0.22 μm filtered seawater within rectangular vessels ranging in dimensions from 4.0 × 8.0 × 2.0 to 25.5 × 30.5 × 18.5 (width × height × depth, cm) and volumes from 50 to 14 000 ml. Vessel choice depended upon medusa diameter; small vessels used for *Linuche unguiculata*, while *Stomolophus meleagris* and *Cyanea capillata* required larger vessels. A field counter labelled each sequential VHS video frame (1/60 s per field) in order to provide temporal information. Spatial characteristics of the optical field were determined from scale bars periodically included in the recordings.

Kinematic data were collected for an individual medusa of all three species studied. Alterations in bell shape were quantified by the fineness ratio, F, where

$$F = h/d$$

and h is bell height while d is bell diameter. Bell diameter was measured as the distance between two opposite sides of the bell margin. Instantaneous fineness ratio, F_i, represents the fineness ratio during the midpoint of an interval used for measurement of medusa velocity. F_i was determined to quantify variations in bell morphology during the pulsation cycle. The fineness ratio of the bell at rest in its uncontracted state corresponds closely to the minimum F_i value, whereas maximum F_i corresponds to full bell contraction.

Medusa motion was measured from sequential changes in position (x) of the anterior-most point of the exumbrellar surface over uniform time intervals (t). This was a simple and rapid measurement for *Linuche unguiculata* and *Stomolophus meleagris* because bell pulsation does not significantly alter the shape of the anterior bell. The anterior-most point of the bell was therefore an accurate estimator of position for these species. For *Cyanea capillata*, however, the anterior bell may be depressed downward during bell recovery. If the bulk of the medusa continues forward during this interval, then use of the anterior-most bell position could be an inappropriate indicator of overall medusa position. In order to avoid introducing bias into the position data due to the complex motion of *C. capillata*, we measured changes in the center of mass of the oral arms with successive digital images (Optimas, Bioscan Inc.) of a swimming sequence by *C. capillata*. The time intervals between position measurement were two fields (1/30 s) for *S. meleagris* and *L. unguiculata* and five fields (1/12 s) for *C. capillata*. These differences in the interval lengths were due to differences in pulsation rate among species. Motion only within the two-dimensional viewing field was assured by using a sequence in which bell orientation was level and the medusa swam from bottom to top of the viewing field.

The velocity (u) for a specific time interval (i) was calculated as an average according to the formula

$$u_i = \frac{x_{i+1} - x_{i-1}}{2t}.$$

Reynolds number (Re) was calculated as

$$Re = \frac{du}{v},$$

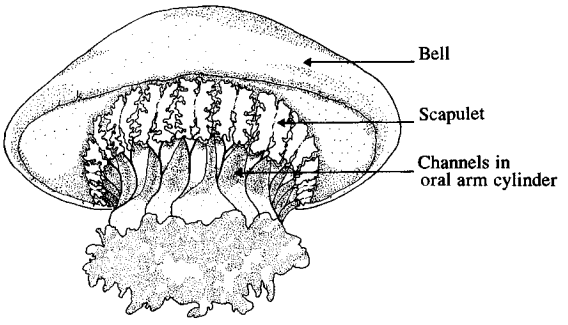

Fig. 1 *Stomolophus meleagris*. Body features relating to flow and prey capture

where u is medusa velocity and v is the kinematic viscosity of seawater.

Qualitative information on flow patterns surrounding swimming medusae was based on motion of tracer particles or fluorescein dye. Mixed natural plankton captured with a 333 μm mesh net or 4-d-old *Artemia* sp. nauplii (0.3 to 0.6 mm length) served both as tracer particles and as prey. *Artemia* sp. nauplii were visibly entrained in flow surrounding the medusae and all three species readily captured and ingested *Artemia* sp. nauplii. Likewise, consumption of live plankton by medusae was observed in order to determine principal capture surfaces. Dye was used to observe details of flow separation and vortex formation not readily apparent using particles. While kinematic profiles were collected from a single, representative swimming sequence, flow diagrams were synthesized from observations of several individuals of each species.

Results

The interactions between fluid motions and body morphology were different for each of the three species of medusae examined. Therefore, each species is considered separately, and a description of important morphological characteristics precedes flow and kinematic data for each species.

Stomolophus meleagris

The bell of *Stomolophus meleagris* is thick and almost rigid except near the margin. Beneath the bell, the body is a complex of fused, channeled surfaces and elaborate structures active in prey capture (Fig. 1). The oral arm cylinder is formed by the lateral coalescence of eight adradial oral arms and hangs from the center of the bell. Deep grooves extend along the length of the oral cylinder and end in the bifurcated, flanged base of the cylinder. The upper portion of the cylinder is elaborated into scapulets which line the ridges of the cylinder under the medusa bell. The active prey capture sites are multiple mouths surrounded by small, nematocyst bearing extensions of the oral arm wall. Many of these small mouths are located on the scapulets and the distal end of the oral arm cylinder. More detailed descriptions of morphology and development are given by Mayer (1910) and Larson (1991).

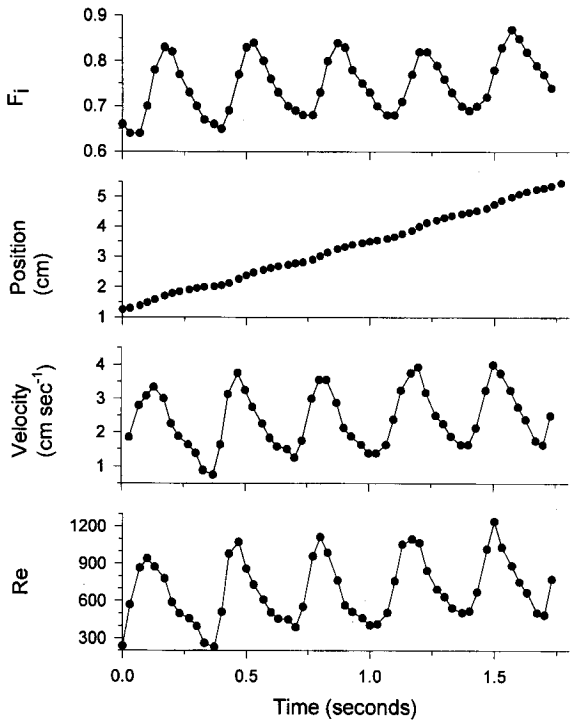

Fig. 2 *Stomolophus meleagris.* Instantaneous bell fineness (F_i), vertical position of the medusa in the water column, velocity and Reynolds number (*Re*) determined from a swimming medusa, 3.3 cm diameter

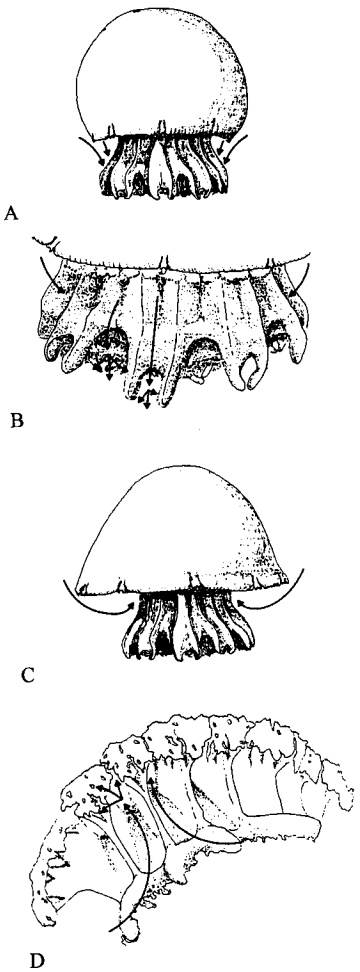

Fig. 3 *Stomolophus meleagris.* Patterns of fluid flow through capture structures. **A** Large scale flow pattern during the power stroke. **B** Flow along and through the distal end of the oral arm cylinder during the power stroke. **C** Large scale flow pattern during the recovery stroke. **D** Flow through proximal portion of the oral arm cylinder and scapulets during the recovery stroke. View is along the oral–aboral axis

Swimming, and resultant fluid motions past the medusa's body, were generated by bell contraction. Contraction of the bell, measured as increased F_i, forced fluid out from the subumbrellar space and resulted in thrust production and increased forward velocity of the medusa (Fig. 2). Velocity increases actually preceded increases in F_i because muscle contractions started at mid-bell and moved towards the bell margin. Water expulsion from the bell began before the widest portion of the bell, the bell margin, contracted. Since F_i is the ratio of length to diameter, this pattern of bell contraction resulted in forward thrust starting while the bell was widest (lowest F_i). However, maximum velocity was attained after the muscle contraction propagated through the bell margin. Hence, peak F_i and velocity measurements coincided. Refilling of the subumbrellar space with fluid during the recovery phase of the pulsation cycle did not result in negative velocities or cessation of the forward progress of the medusa through the water (Fig. 2). In other words, forward progress was always positive, even during periods with no thrust production. The relatively high Re over most of the pulsation cycle ($Re = 684 \pm 254$) indicated that fluid flow around the medusa was dominated by inertial forces. The 3.32 cm diameter medusa illustrated (Fig. 2) completed three pulsation cycles s^{-1}.

Qualitatively important interactions involving fluid motions and feeding for *Stomolophus meleagris* are also illustrated (Fig. 3). During bell contraction, fluid expelled from the bell cavity, as well as fluid entrained from adjacent to the bell margin, was pushed downward along the channeled surface of the oral arm cylinder and through the flanged base of the cylinder. The distal surface of the cylinder base is elaborated into numerous small mouths that are active in prey capture. Consequently, bell contraction jets water through the distal capture surface of *S. meleagris*. As also noted by Larson (1991), we observed that the turbulent wake behind the oral arm cylinder often brought entrained prey into contact with the distal surface of the oral arm cylinder.

The recovery phase of the pulsation cycle resulted in an inward flux of fluid into the expanded bell cavity (Fig. 3C). Part of the influx of fluid, and prey entrained in that fluid flow (Fig. 3D), passed proximally, up the channeled oral arm cylinder, and through the scapulets. Because the scapulets are covered with

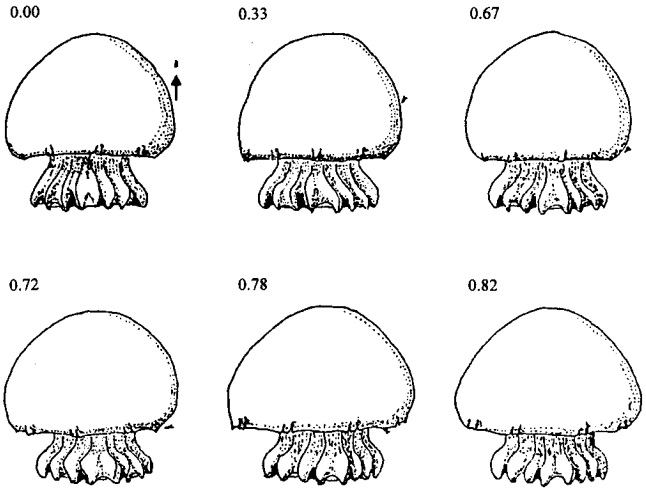

Fig. 4 *Stomolophus meleagris.* Entrainment of a 4-d-old *Artemia* sp. nauplius into the flow surrounding a 3.3 cm diameter medusa. The elapsed time in seconds is shown above each image. *Arrow* in first frame (time = 0.00 s) indicates initial prey location. Relative sizes of medusa and prey drawn to scale. First three frames depict the relative position of the medusa and at the end of three successive power strokes. Transport of prey into the subumbrellar space occurred during the recovery phase of the third pulsation (time = 0.72 to 0.82 s, Frames 4 to 6). Actual prey capture on the scapulets was obscured by the bell but the nauplius did not exit the subumbrellar space and was assumed captured

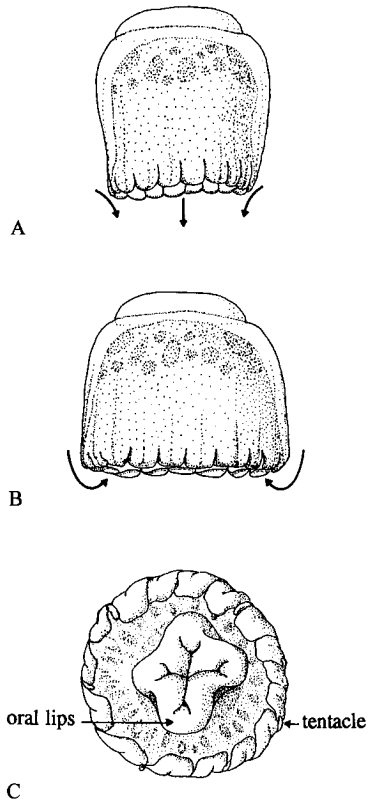

Fig. 5 *Linuche unguiculata.* Fluid flow and bell position during **A** bell contraction and **B** bell relaxation. **C** View from oral end, towards the subumbrellar surface, during bell relaxation

nematocyst bearing tissue, prey entrained in this flow were sieved out of the fluid and retained on the scapulets. Thus, while bell contraction pushes prey onto distal capture surfaces of *S. meleagris*, the recovery stroke pulls prey into the proximal capture surfaces. Most prey captures that we observed took place on the proximal surfaces during the recovery stroke (Fig. 4). This observation may be biased, however, because prey paths into the bell were more visible than prey paths near the distal end of the oral arm cylinder. The consistently positive forward progress of the medusa through the fluid had the effect of positioning the medusa in a new location for each power and recovery stroke and thereby prevented re-entrainment of previously sieved fluid.

Linuche unguiculata

The relaxed bell form of *Linuche unguiculata* is bluntly prolate (Fig. 5). Bell contraction involves the region extending from approximately mid-bell to the bell margin. This area of the bell is underlain by the coronal muscle fields which power bell contraction. The tentacles of *L. unguiculata* are short, club-shaped, and non-contractile. The tentacles are inserted between the marginal lappets. The lappets are thrust outwards during bell contraction and bend inwards during the recovery stroke (Fig. 5). The manubrium extends distally about half the length of the bell and terminates in a large, simple mouth without elaboration into oral arms. A more detailed description of the morphology and development of *L. unguiculata* can be found in Mayer (1910).

Bell contractions by *Linuche unguiculata* were rapid (2.5 pulsations s^{-1} for a 1.5 cm diameter medusa, Fig. 6) and resulted in sharp velocity increases. Velocity declined rapidly during the recovery stroke and remained low and relatively constant during a coasting phase between pulsation cycles. As with *Stomolophus meleagris*, changes in position and resultant velocities were always positive. The profile illustrated in Fig. 6 depicts motion from rest starting midway through the first power stroke. After the third bell contraction, cyclic velocity variations were consistent and Re ranged from 123 to 386.

Entrainment of fluid, and associated prey, occurred as a result of the bell pulsation cycle. During the power stroke, bell contraction forced water out of the bell cavity and created forward thrust for the medusa. During the recovery stroke, water flowed past the bell margin and into the subumbrellar space. Prey entrained in this flow were brought into contact with marginal lappets, the oral arms or the subumbrellar wall (Fig. 5). Capture of a copepod by *Linuche unguiculata* is illustrated in Fig. 7. All captures occurred

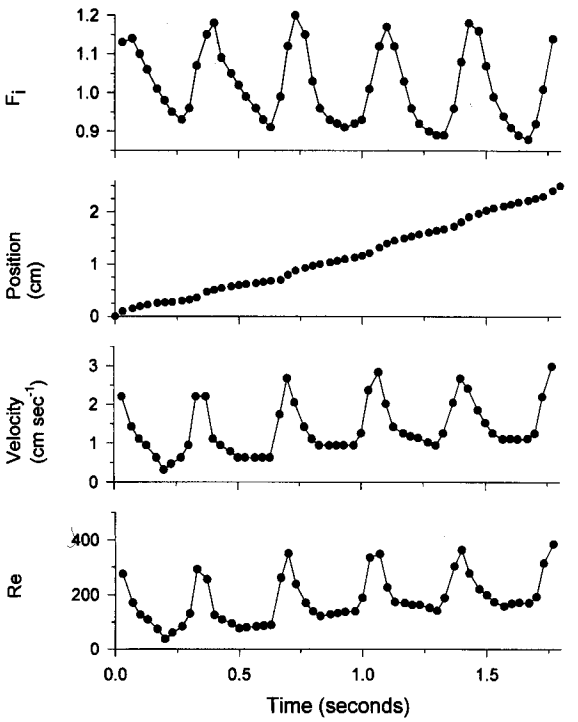

Fig. 6 *Linuche unguiculata.* Instantaneous bell fineness (F_i), vertical position of the medusa in the water column, velocity and Reynolds number (*Re*) determined from a swimming medusa, 1.5 cm diameter

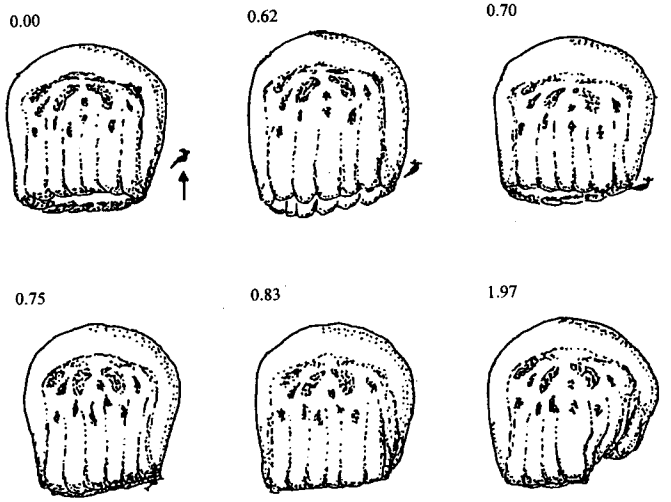

Fig. 7 *Linuche unguiculata.* Capture of a copepod by a 1.5 cm diameter medusa. The elapsed time in seconds is shown above each image. *Arrow* in first frame (time = 0.00 s) indicates initial prey location. Relative sizes of medusa and prey drawn to scale. Note that transport of the prey to the medusa's capture surface occurred during the recovery stroke (time = 0.70 s) and bell crumpling, indicating prey capture (time = 0.83 s) interrupted further bell pulsation. After prey capture, the bell remained crumpled for 12 s before regular bell pulsation and forward motion resumed

within the subumbrellar cavity and were followed by a crumpling response (Fig. 7). Only prey that were adjacent to the bell margin were actually captured. Plankton further from the bell margin were also entrained into the subumbrellar cavity but were generally expelled with the next bell contraction, possibly before contacting the interior capture surfaces. These plankton often resumed normal swimming behavior after expulsion from the subumbrellar space. We did not observe any prey captures on the tentacles.

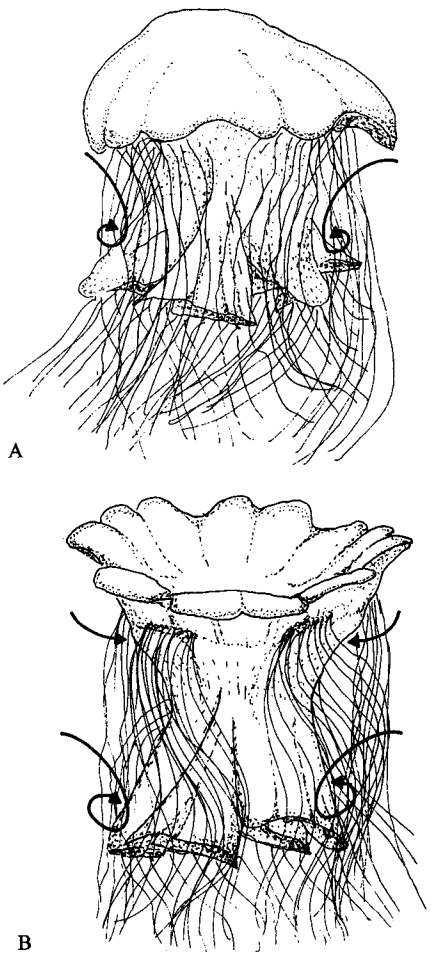

Fig. 8 *Cyanea capillata.* Fluid flow and bell position during **A** bell contraction and **B** bell relaxation

Cyanea capillata

The umbrella of *Cyanea capillata* is broad and flat (Fig. 8). As described by Gladfelter (1972), the umbrella consists of two principal functional units: a central disc and a lateral outer region. The outer region can be divided into eight major lobes, each consisting of two fused, broad, marginal lappets. Between the lappets on each lobe lies the rhopalium, or sensory organ. Eight clusters of tentacles arise from the subumbrellar surfaces between the major marginal lobes. The tentacles hang in variable lengths below swimming medusae and may be contracted at the subumbrellar surface or extended many body diameters behind the medusa. The

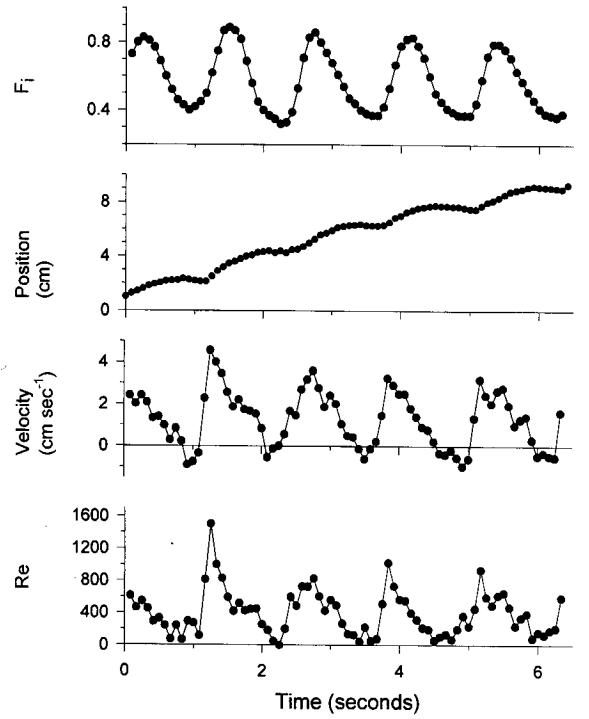

Fig. 9 *Cyanea capillata.* Instantaneous bell fineness (F_i), vertical position of the medusa in the water column, velocity and Reynolds number (*Re*) determined from a swimming medusa, 3.9 cm diameter

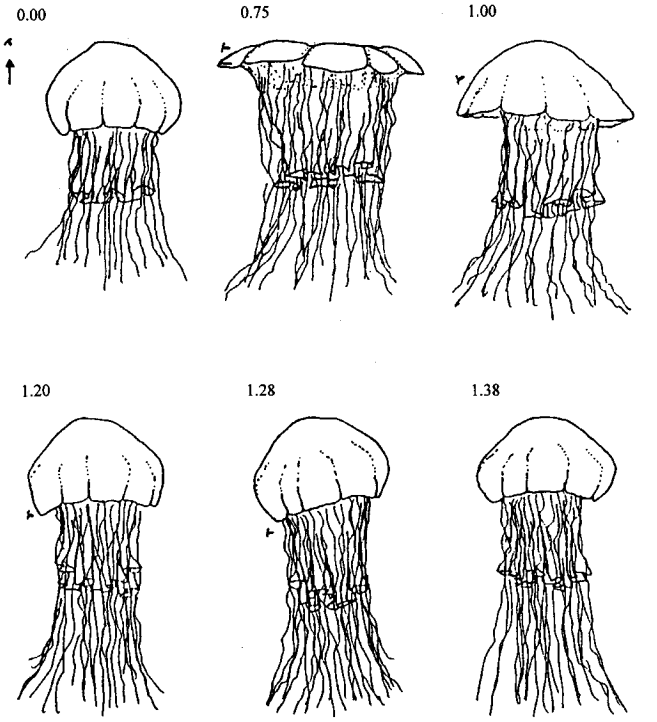

Fig. 10 *Cyanea capillata.* Capture of a 4-d-old *Artemia* sp. nauplius by a 4.5 cm diameter medusa. The elapsed time in seconds is shown above each image. *Arrow* in first frame (time = 0.00 s) indicates initial prey location. Relative sizes of medusa and prey drawn to scale. Prey entrainment started during the contraction phase of bell pulsation (time = 0.75 s) and resulted in prey capture on the tentacles in the far right frame (time = 1.38 s)

four oral arms are elaborated into highly folded lips which hang downward from the bell. More detailed descriptions of the morphology of *C. capillata* are given by Mayer (1910), Russell (1970) and Gladfelter (1972).

Bell pulsation by *Cyanea capillata* involved contraction of the marginal lobes downward, followed by relaxation of the lobes and their return to a concave orientation relative to the central disc (Fig. 8). During the recovery stroke, forward motion ceased, and the center of mass of the medusa actually moved backwards, resulting in negative velocities. The onset of the contraction phase coincided closely with increased velocity and forward progress (Fig. 9). The alternation between peak velocities during the power stroke and negative velocities during recovery resulted in Re variations of 0 to 1500 over the course of the pulsation cycle.

The influence of this unsteady motion on fluid flows was examined with dye and is illustrated (Fig. 8). During the power stroke, water entrained from adjacent to the bell margin was shed as a series of vortices which travelled distally through the medusa's tentacles. During the recovery stroke, as the marginal lobes returned to an upright position, water was drawn inward towards the subumbrellar surface and through the tentacles near the bell margin. The following power stroke thrust the bell forward and resulted in another set of shed vortices. A medusa swimming in a straight path often left two sets of vortices visible in its wake. The structure of previously created vortices dissipated rapidly in the still water of the filming vessels. The net result of the pulsed flow was that the medusa created an unsteady flow of fluid and entrained particles from the bell towards its tentacles. Prey capture occurred near the bell (Fig. 10) or along the length of the tentacles and oral arms as they were dragged through the wake of the medusa. Tentacular captures were followed by contraction of the tentacle(s) holding prey and transfer of prey from the tentacle(s) to the oral arms, where ingestion occurred.

Discussion

Previous research on planktonic scyphomedusan feeding makes little mention of relationships between prey capture and fluid motions created during bell pulsation (exceptions include the studies by Larson 1991, Costello 1992 and Costello and Colin 1994). This may be largely due to temporal and spatial limitations of methods used by previous investigators. First, prey capture is often too rapid for unassisted direct observation. Many medusae complete several pulsations per

second (Figs. 2, 6), and the speed at which prey are entrained and captured exceeds the temporal resolution of the unaided human eye. For example, transport of prey to capture surfaces takes 0.2 to 0.3 s for *Stomolophus meleagris* (Fig. 4) and *Linuche unguiculata* (Fig. 7). The slower pulsation rate of *Cyanea capillata* resulted in a slightly longer duration for prey capture events (<0.75 s, Fig. 10). Second, scyphomedusae are often large relative to their prey, and simultaneous observation of both is difficult. For example, Larson (1991) found that the majority of prey selected by *S. meleagris* (mean bell heights 28 to 82 mm) were 0.2 to 0.4 mm long. Likewise, Fancett (1988) found that while *C. capillata* reached bell diameters of close to 100 mm, their principal prey items were less than 5 mm in length. These large disparities between predator and prey dimensions make simultaneous observation of activities by both during feeding difficult to resolve (note relative medusa and prey dimensions in Figs. 4, 7, 10). For *S. meleagris* and *C. capillata*, we used medusae that possessed morphologies characteristic of adult medusae but were still small enough to simultaneously observe both medusae and prey. We used fully developed *L. unguiculata* medusae because sexually mature adults are relatively small, generally less that 2.5 cm in diameter. The applicability of these results for *S. meleagris* and *C. capillata* may be limited due to our use of comparatively small individuals. However, since *S. meleagris* (Larson 1991) and *C. capillata* (Fancett 1988) exhibit consistent prey selection patterns over broad ranges in bell diameter, it is probable that the mechanisms we describe are also applicable over broad ranges in bell diameter. This pattern has previously been documented for *Aurelia aurita* (Costello and Colin 1994; Sullivan et al. 1994). Video helped in this study because inexpensive, repeated direct observations could be made on time and space scales appropriate to these events.

Our results using three scyphomedusan species with different morphologies from different orders suggests that the use of bell pulsation-induced flows for entrainment and capture of prey is widely developed among the scyphomedusae. The three species studied do not simply drift into their prey, as do hydrozoans such as the siphonophore *Physalia physalis*. Instead, fluid motions created during bell pulsation serve both to propel the medusae forward and to entrain prey for feeding. After the ephyral stage, all of these medusae live in flows characterized by $Re > 10^2$ (Figs. 2, 6, 9). Consequently, the flows around these medusan bodies are dominated by inertial forces, as are the prey entrained in these flows. As illustrated by *Stomolophus meleagris*, *Linuche unguiculata* and *Cyanea capillata*, medusae that have evolved divergent morphologies are able to use different components of the flow resulting from bell pulsation. Feeding by *S. meleagris* demonstrates that flow need not pass through tentacles in order to be utilized for prey capture. Like most other rhizostomes, *S. meleagris* has no tentacles. Instead, its body is elaborated into a form that channels and sieves fluid motions created by bell pulsation. Both the power and recovery strokes are utilized; capture surfaces are appropriately located on different body parts to utilize fluid motions created by each portion of the pulsation cycle. Data presented here concur with a previous description (Larson 1991) of *S. meleagris* as a filter feeder which captures prey brought by pulsation-induced flow to capture surfaces. The channel and sieve structure of *S. meleagris* is not unique among rhizostome scyphomedusae. It is probable that other planktonic rhizostomes, such as members of the genera *Rhopilema* and *Rhizostoma*, may capture prey in a similar manner. Tentacles are either absent or extremely reduced in these medusae while their body forms are channeled and elaborated in ways similar to *S. meleagris* (Mayer 1910). The rhizostome medusae are thought to have evolved from semaeostome ancestors (Russell 1970) and may represent a taxon whose specialized morphologies and pulsation-induced flows are well adapted for prey capture.

Tentaculate scyphomedusae differ in their use of pulsation-induced flow for prey capture. The role of the short tentacles of *Linuche unguiculata* in prey capture is not clear. Our observations do indicate, however, that prey capture depends upon entrainment and transport of prey during the recovery stroke. *Aurelia aurita*, a semaeostome with moderately long tentacles, generally not longer than one bell diameter, also depends upon fluid motion during the recovery stroke to entrain and capture prey (Costello and Colin 1994). This may indicate that species with short to moderate length tentacles, such as *L. unguiculata* and *A. aurita*, use primarily the recovery stroke flow for prey capture. The vortices created during the power stroke are more useful to medusae with long, trailing tentacle masses, such as *Cyanea capillata*. In the latter case, the tentacles are long enough to intercept the power stroke vortices, and the trailing tentacles can be dragged through the wake behind the swimming medusae. The importance of flow-related prey capture for overall prey intake by *C. capillata* remains unresolved, however, because the long tentacles, and often winding swimming path of *C. capillata*, may cause much of the tentacle mass to lie outside of the flow created by bell pulsation or beyond the area where flow is strong enough to entrain prey. Under these circumstances, the long tentacles may function as much to ambush cruising prey as to sieve flow caused by bell pulsation.

The mechanics of prey capture by scyphomedusae have important ecological implications for planktonic communities in which these medusae are significant predators. If flow generated during swimming is the underlying mechanism determining prey encounter, then prey selection (the prey consumed as compared to the prey available in the plankton) should depend upon prey vulnerability to entrainment in the flow created by

swimming medusae. Therefore, prey escape characteristics, particularly swimming velocities, should be important variables influencing medusan prey selection. Medusae that use flow to capture prey are cruising predators and would be predicted to capture slowly moving prey. Similarly, medusae that sit and wait for prey to swim into their tentacles are ambush predators and would be predicted to capture rapidly swimming prey (Gerritsen and Strickler 1977). Based on this logic, Costello and Colin (1994) predicted selection patterns for *Aurelia aurita* by comparing flow velocities created by swimming medusae with escape velocities of available prey. Independently, Sullivan et al. (1994) found that prey selection patterns of *A. aurita* were largely consistent with these predictions. While this pattern has become clear for *A. aurita*, there are no similar data for most other scyphomedusae. Field prey selection data are not available for *Linuche unguiculata*, although Larson (1979) found that *L. unguiculata* used its lappets to capture microcrustaceans and copepods in the laboratory. *Stomolophus meleagris* and *Cyanea capillata* are unusual among scyphomedusae because details of prey selection by field populations are available. Larson (1991) found that weak or non-swimming prey such as bivalve veligers, fish eggs, larvaceans and tintinnids were selected by *S. meleagris* more frequently than faster swimming prey, such as calanoid and cyclopoid copepods. As with *A. aurita*, it is probable that the faster species escape the flow used for feeding by *S. meleagris*. Similarly, Fancett (1988) found that *C. capillata* selected against all copepods and for slower moving prey such as fish eggs and yolk-sac larvae, the cladoceran *Podon* sp., and larvaceans. Feeding rates of *C. capillata* on later stage fish larvae, which are more capable of escape (Bailey and Batty 1983; Bailey and Yen 1983), were much lower than on eggs and early stage larvae (Fancett 1988). These results suggest that prey selection by field populations of these scyphomedusae are consistent with predictions arising from flow-based prey encounter mechanisms. Whether possessing elongate tentacles or other body modification for prey capture, these scyphomedusae most probably function as cruising predators, relying upon flow created during bell pulsation to bring prey to their capture surfaces. The impact of these predators on any particular planktonic community will depend upon medusan flow field characteristics, prey escape abilities, and physical factors, such as small-scale turbulence, which might affect predator or prey.

Acknowledgements We are grateful to several colleagues for providing us with medusae from diverse locations. P. Kremer and M. Montgomery of the University of Southern California sent *Linuche unguiculata* from the Bahamas, and D. Allen of Baruch Institute, University of South Carolina shipped us *Stomolophus meleagris* from South Carolina, USA. We thank S.H. Costello for assistance with figure preparation. Financial support for this research was provided by the National Science Foundation (OCE 9103309 to JHC).

References

Bailey KM, Batty RS (1983) A laboratory study of predation by *Aurelia aurita* on larval herring (*Clupea harengus*): experimental observations compared with model predictions. Mar Biol 72: 295–301

Bailey KM, Yen J (1983) Predation by a carnivorous marine copepod, *Euchaeta elongata* Esterly, on eggs and larvae of the Pacific hake, *Merluccius productus*. J Plankton Res 5: 71–82

Costello JH (1992) Foraging energetics in hydromedusae. Scientia marina 56: 185–191

Costello JH, Colin SP (1994) Morphology, fluid motion and predation by the scyphomedusa *Aurelia aurita*. Mar Biol 121: 327–334

Fancett MS (1988) Diet and prey selectivity of scyphomedusae from Port Phillip Bay, Australia. Mar Biol 98: 503–509

Gerritsen J, Strickler JR (1977) Encounter probabilities and community structure in zooplankton: a mathematical model. J Fish Res Bd Can 34: 73–82

Gladfelter WB (1972) Structure and function of the locomotory system of the scyphomedusa *Cyanea capillata*. Mar Biol 14: 150–160

Larson RJ (1979) Feeding in coronate medusae (Class Scyphozoa, Order *Coronatae*). Mar Behav Physiol 6: 123–129

Larson RJ (1991) Diet, prey selection and daily ration of *Stomolophus meleagris*, a filter-feeding scyphomedusa from the NE Gulf of Mexico. Estuar cstl Shelf Sci 32: 511–525

Lindahl O, Hernroth L (1983) Phyto-zooplankton community in coastal waters of western Sweden – an ecosystem off balance? Mar Ecol Prog Ser 10: 119–126

Madin LP (1988) Feeding behavior of tentaculate predators: in situ observations and a conceptual model. Bull mar Sci 43: 413–429

Matsakis S, Conover RS (1991) Abundance and feeding of medusae and their potential impact as predators on other zooplankton in Bedford Basin (Nova Scotia, Canada) during Spring. Can J Fish aquat Sciences 48: 1419–1430

Mayer AG (1910) Medusae of the world. III. The Scyphomedusae. Publication of the Carnegie Institute of Washington, Washington DC

Mills CB (1981) Diversity of swimming behaviors in hydromedusae as related to feeding and utilization of space. Mar Biol 64: 185–189

Moller H (1980a) Scyphomedusae as predators and food competitors of larval fish. Meeresforsch Rep mar Res (Ber dt wiss Kommn Meeresforsch) 28: 90–100

Moller H (1980b) Population dynamics of *Aurelia aurita* medusae in Kiel Bight, Germany (FRG). Mar Biol 60: 123–128

Moller H (1984) Reduction of a larval herring population by a jellyfish predator. Science, NY 224: 621–622

Purcell JE (1992) Effects of predation by the scyphomedusan *Chrysaora quinquecirrha* on zooplankton populations in Chesapeake Bay, USA. Mar Ecol Prog Ser 87: 65–76

Russell FS (1970) The medusae of the British Isles. II. Pelagic Scyphozoa. Cambridge University Press, Cambridge, UK

Sullivan BK, Garcia RJ, McPhee-Klein G (1994) Prey selection by the scyphomedusan predator *Aurelia aurita*. Mar Biol 121: 335–341